

Simultaneous Eccentricity and Drift Rate Control

Charles F. Gartrell*

General Research Corporation, McLean, Va.

A disturbing force due to solar pressure is shown to cause comparatively large variations in eccentricity. This phenomenon obviates the traditional approach to east-west stationkeeping when longitude control boxes are on the order of ± 0.1 deg. A control theory is presented which accounts for annual and satellite variations in simultaneously controlling eccentricity and drift rate. It is also shown that a continuous thrusting scheme is a viable alternative to controlling eccentricity for large geosynchronous platforms of the future.

Introduction

WHEN an operational geosynchronous equatorial orbit is nearly circular (i.e., $e \ll 0.01$), then a portion of eccentricity motion is due to the ever-present solar pressure. This effect has largely been ignored in the traditional approach to east-west stationkeeping. Problems with unintentional transmission interference has prompted the International Radio Consultative Committee Study Group 4 to change the limit for geosynchronous communication satellites movement of ± 0.5 deg about a nominal position to ± 0.1 deg.¹ Further restrictions have occurred due to individual carrier concern over the quality of transmissions on their service area fringes (one carrier is currently using ± 0.07 deg and another plans to use ± 0.03 deg when they become operational). Consequently, the requirements on the space segment of satellite communications have become more stringent with typical longitude control boxes having slipped below ± 0.1 deg. In this regime, the daily change in eccentricity due to solar pressure, as will be shown, causes a daily excursion in longitude that is a significant portion of the control box. Consequently, it becomes imperative that eccentricity be controlled through either of two basic approaches. The first randomly keeps eccentricity small; the second utilizes the solar pressure motion to advantage to control not only eccentricity but also longitude, that is, east-west stationkeeping.

Presented herein are the effects of solar pressure on typical communication satellites of today, and the methodology to perform east-west stationkeeping. In addition, an examination is made of the effect of solar pressure upon proposed large geosynchronous platforms.

Solar Pressure and Eccentricity

If P is the solar pressure and A the surface area projected to the solar wind, then the perturbing force \bar{f} per unit mass m upon a satellite is

$$\bar{f} = (-PA/m)\xi \quad (1)$$

where ξ is the unit vector from the satellite to the sun.

Table 1 puts into perspective the range of accelerations upon a spacecraft at geosynchronous orbit. As can be seen, the acceleration due to solar pressure can be smaller than the gravitational accelerations. However, in the longitude control regime of interest (± 0.1 deg and smaller), the daily excursions in longitude due to solar pressure become significant and must be contended with. Furthermore, as the area/mass ratio increases, solar pressure acceleration will become on the order of the Earth gravitational perturbations.

If, instead of the usual Keplerian elements, a change is made to a canonical set, then a pseudovector can be written $\bar{e} = (e \cos \theta, e \sin \theta)$, where e is eccentricity and θ is the longitude of perigee (which shall be defined in more detail later in this paper).² This particular form allows for an elegant representation of perigee motion, permitting polar plots to be made. Utilizing the usual perturbation methods under the restriction of a near-circular orbit produces the time derivative of eccentricity $d\bar{e}/dt$:

$$V(d\bar{e}/dt) = (PA/m) \cos \delta [3 \sin \alpha \cos \alpha \hat{x} + (1 + \sin^2 \alpha) \hat{y}] \quad (2)$$

where δ is the sun's declination, V is the orbital velocity, and α is the right ascension relative to the intersection of the daily mean solar meridian and the equator (i.e., daily mean solar longitude). This coordinate system is illustrated in Fig. 1. Equation (1) implies that the solar pressure is a constant at all times (and that A/M is constant—in reality, the ratio will vary slowly with time). Averaged over a single orbit, this is true; however, the Earth's slightly eccentric orbit causes annual variations, and momentum transfer makes the apparent pressure greater than expected. Thus, the solar pressure term can be written as

$$P = \beta P_0 (1 + R_m \cos \eta) \quad (3)$$

where P_0 , the nominal solar pressure, is equal to 4.81×10^{-8} dyne/cm², β is the annual variation in this pressure from Fig. 2, R_m is the orbital mean reflectivity of the satellite materials, and η the angle between the surface normal and the sun vector ξ . The mean reflectivity can be estimated by

$$R_m = \frac{1}{A} \sum_i A_i R_i$$

Table 1 Accelerations (m/s²) at geosynchronous equatorial orbit

Earth gravitational:	
First order	2.24×10^{-1}
J_{20} perturbation	2.78×10^{-6}
Solar gravitational perturbation	$< 4 \times 10^{-7}$
Lunar gravitational perturbation	$< 9 \times 10^{-7}$
Solar pressure (not including momentum transfer, etc.):	
$A/M = 0.01$ m ² /kg	4.81×10^{-8}
$A/M = 0.05$ m ² /kg	2.41×10^{-7}
$A/M = 0.1$ m ² /kg	4.81×10^{-7}
$A/M = 0.5$ m ² /kg	2.41×10^{-6}

Received May 2, 1980; revision received Aug. 25, 1980. Copyright © 1980 by C.F. Gartrell. Published by the American Institute of Aeronautics and Astronautics with permission.

*Senior Engineer, Washington Operations. Member AIAA.

where A_i , R_i are the area and reflectivity, respectively, for each type of material (thermal blanket, solar cells, etc.) utilized upon the surface of the satellite.

The angle γ , as shown in Fig. 3, is representative of the portion of the orbit that is sunlit during a solar day. Consequently, Eq. (2) can be integrated over one solar day to yield the total daily effect upon eccentricity

$$V\delta\vec{e} = \int_{-\gamma}^{\gamma} \frac{PA}{m} [3\hat{x}\sin\alpha\cos\alpha + (1 + \sin^2\alpha)\hat{y}] \cos\delta dt$$

but $dt = \dot{\alpha}^{-1} d\alpha$, and $PA/m\dot{\alpha}$ is a constant over one orbit, so

$$V\delta\vec{e} = \hat{y} (PA/m\dot{\alpha}) \cos\delta [3\gamma - (\sin 2\gamma)/2] \quad (4)$$

Equation (3) can now be introduced, and will yield the result

$$\delta\vec{e} = \hat{y} [\beta P_0 A (1 + R_m \cos\eta) / Vm\dot{\alpha}] \cos\delta [3\gamma - (\sin 2\gamma)/2] \quad (5)$$

Since eclipses are experienced semiannually ($P=0$ during these periods), the portion of the orbit that is sunlit varies throughout the year from as little as 342.936 deg at mideclipse

to as much as 360.9856 deg during noneclipse seasons. The maximum value for the sunlit portion of the orbit (360.9856 deg) exceeds 360 deg as the integration is occurring over a mean solar day (86,400 s) whereas the orbital period is a sidereal day (86,164.1 s). The angle γ can be determined with the aid of Fig. 4. The satellite-independent portion of Eq. (5) can easily be determined as a function of time of year. Figure 5 is a plot of this functional behavior. Note that this is a plot of

$$g(t) = [Vm/A(1 + R_m \cos\eta(t))] \delta e(t)$$

a function of the time of year.

As the sun rotates about the Earth in an equatorial inertial space, the direction of the eccentricity vector will also rotate. Consequently, if the right ascension of perigee is aligned with the mean solar meridian, then the eccentricity vector of the orbit will also rotate with the sun. In addition, if the value of eccentricity is made equal to $\delta e / [\sin(2\pi/365.25)]$, the eccentricity vector will rotate in a circle with a radius of the same value, a "steady-state" eccentricity (e_{ss}).

Typical Eccentricity Motion

In order to study these results in detail, several typical examples are considered below. From Eq. (5), the key satellite-dependent parameters are area/mass ratio (A/m), mean reflectivity (R_m), and angle (η). For simplicity, the velocity under consideration is that associated with geosynchronous orbits.

The typical communication satellite has fallen into three general types of attitude control configurations: dual spin control, momentum bias control, and three-axis active control. Reference 3 contains a good discussion of the various merits of each approach. The dual spin control satellites are typically large massive cylinders, where the projected areas are about 25 m² with masses of nearly 1000 kg. This control technique is a well-proven method and, as a result, a large number of satellites have been in this class. The momentum-bias-controlled satellites have tended to be fairly lightweight, consisting of basically a cube and large solar panels that track the sun. These satellites are typified by projected areas of about 10 m², with masses of about 550 kg. The three-axis active-controlled satellites, on the other hand, have been basically large antennas, with a resultant area of typically 84 m² and a mass of about 1700 kg. Figure 6 illustrates the various control schemes and examples of each type. The three representative area-mass ratios are approximately those for SBS, RCA SATCOM, and ATS-6.

In order to complete the modeling of the daily eccentricity change, the surface material reflectivity and the sun line-surface normal angle must be modeled. For the purposes of this work, a very simple model has been assumed for the

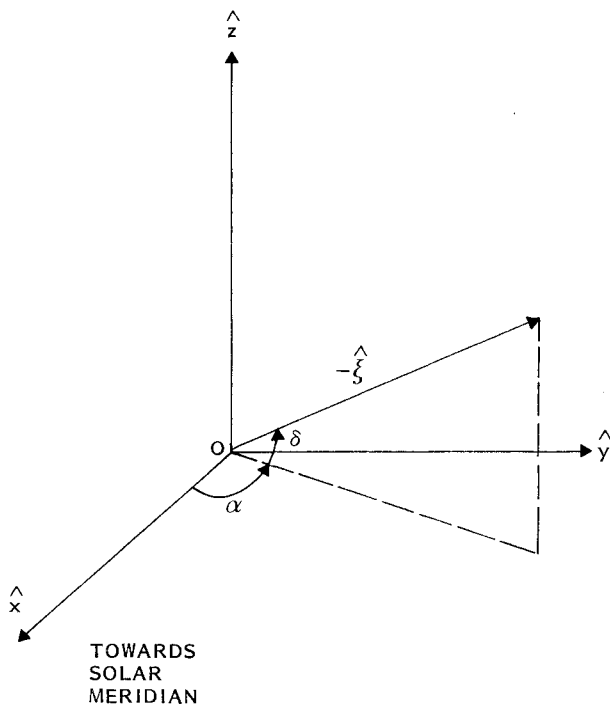


Fig. 1 Eccentricity coordinate system.

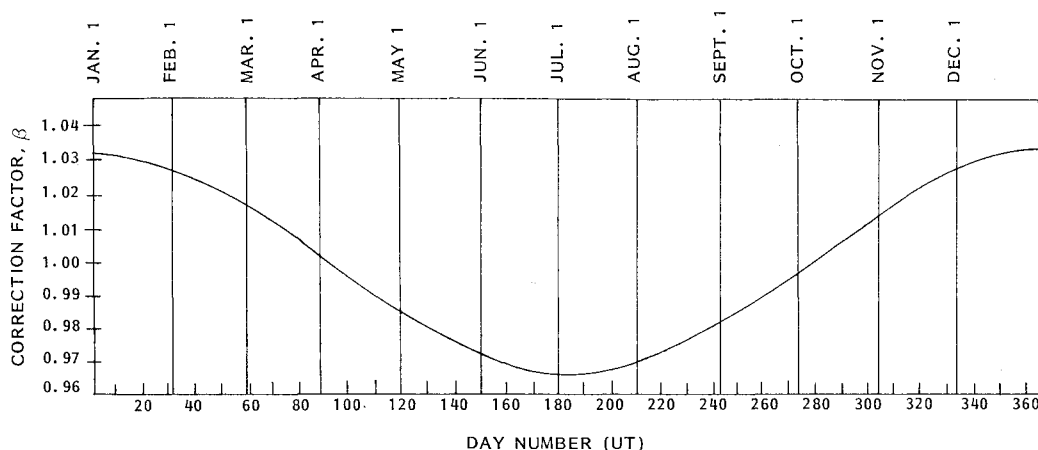


Fig. 2 Annual variation in solar pressure.

surface material: the surface is considered to be composed in part of either solar cells ($R \approx 0.14$), multilayered gold foil thermal blankets ($R \approx 0.85$), or silicon ($R \approx 0.51$); the surface areas A_i are determined by a simple geometric projection into a plane parallel to the spacecraft principal momentum axis and the use of available or derivable dimensions. This model will enable the mean reflectivities to be determined. These are

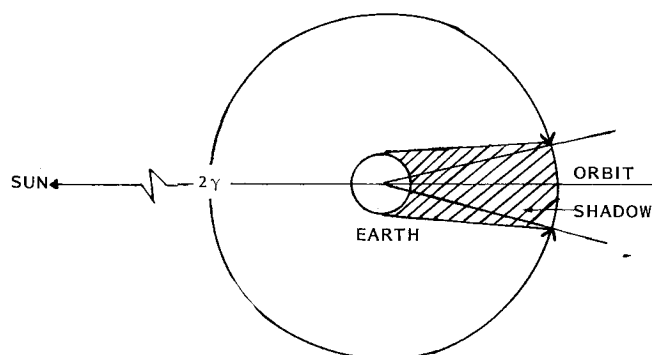


Fig. 3 Portion of orbit sunlit.

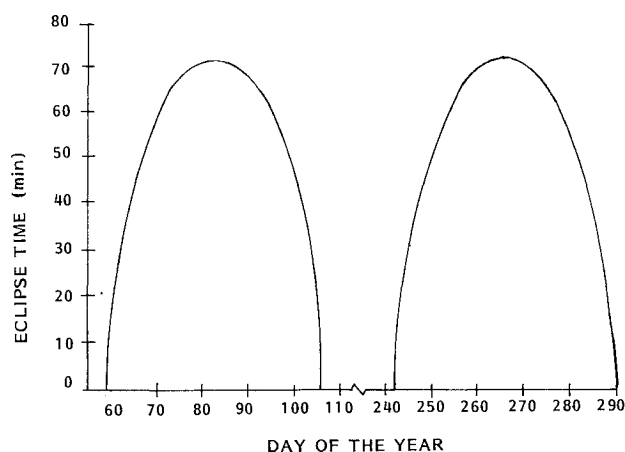


Fig. 4 Eclipse duration for geosynchronous equatorial orbit.

0.14, 0.21, and 0.39, respectively, for each of the three types. As a further simplification, the surface normal is assumed to lie parallel to the equatorial plane, so that the angle η is equal to the sun's declination.

With these assumptions, the daily eccentricity change can be computed for each case as a function of time of year, such as has been done for Fig. 7. The maximum daily excursion in longitude $\delta\lambda$ can be found from the maximum "steady-state" eccentricity e_{ss} in Table 2. These variations will have a significant effect on the actual usable control regime for traditional east-west stationkeeping.⁴ For example, if the control regime is nominally 0.2 deg centered about a station, then the actual total stationkeeping box will become smaller by 0.06-0.08 deg in two of the three cases, to an actual control regime of about 0.13 deg; in the third case, it becomes nearly impossible to perform traditional east-west stationkeeping. Thus, the eccentricity effects become 30% or more of the nominal control box. As a consequence, a stationkeeping method needs to be found which will not only limit these daily longitude excursions, but will also perform east-west stationkeeping.

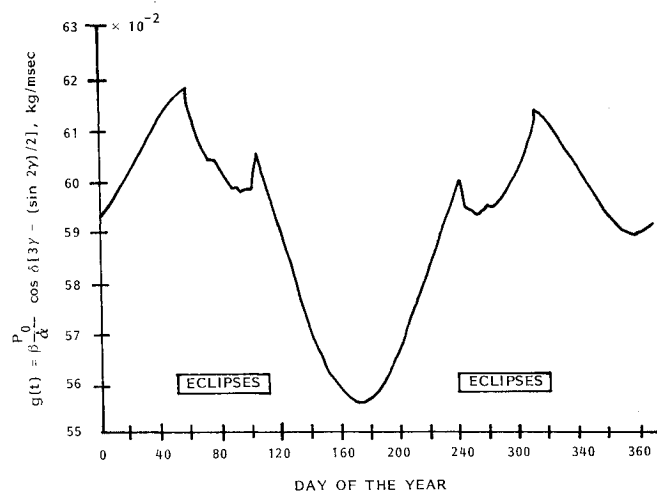
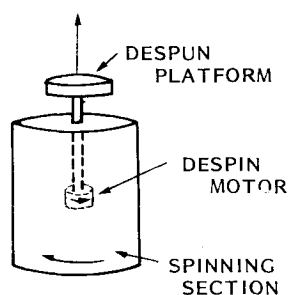


Fig. 5 Normalized daily eccentricity change.

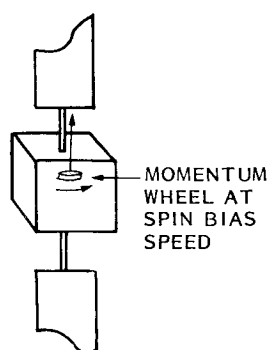
DUAL SPIN CONTROL



A/M ~ 0.026 Typically

Examples: WESTAR
ANIK
COMSTAR
INTELSAT

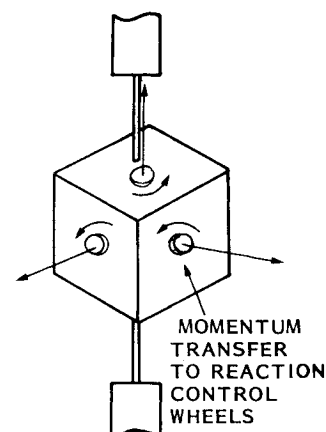
MOMENTUM BIAS CONTROL



A/M ~ 0.018 Typically

Examples: RCA SATCOM
ANIK

THREE-AXIS ACTIVE CONTROL



A/M ~ 0.049 Typically

Examples: ATS-6

Fig. 6 Typical control configurations.

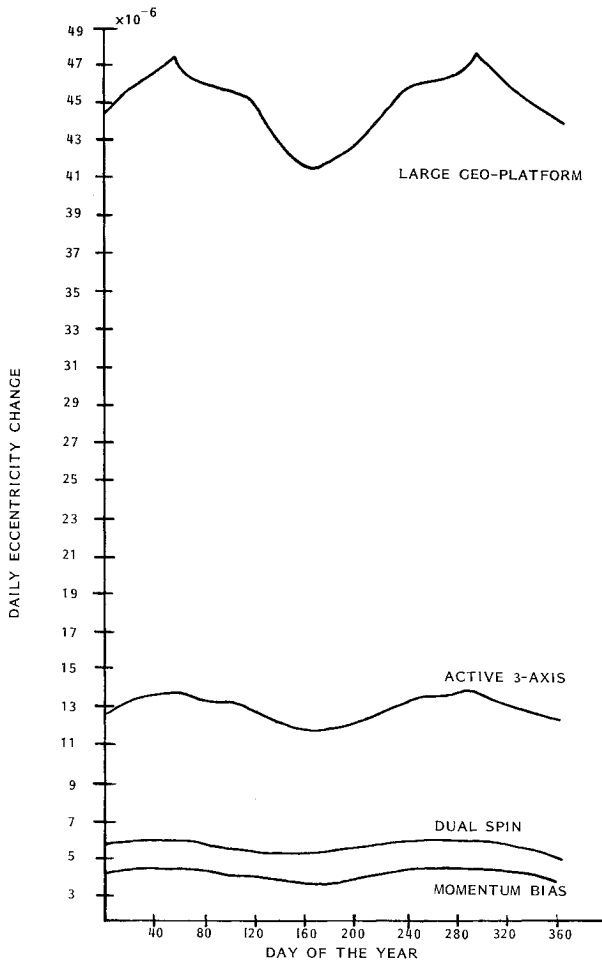


Fig. 7 Daily eccentricity change.

Table 2 Steady-state eccentricity and daily longitude excursion

Control	Max e_{ss}	Max $\delta\lambda$, deg
Dual spin	0.00035	0.08
Momentum bias	0.00025	0.06
Active three-axis	0.00080	0.18

Eccentricity Control

Given an initial eccentricity vector \vec{e}_0 , the intent is to allow the eccentricity to rotate about an arc, 2ψ , such that the magnitude never exceeds the value e_L . For the geosynchronous equatorial orbits, the initial vector can be written as

$$\vec{e}_0 = e_0 \begin{pmatrix} \cos\theta_0 \\ \sin\theta_0 \end{pmatrix}$$

where θ_0 , the longitude of perigee, is defined as the sum of the right ascension of the ascending node Ω_0 , and the argument of perigee ω_0 . The time to go through this arc, 2ψ , is determined by

$$\tau = 365.25\psi/\pi \quad \text{days} \quad (6)$$

It is this time we wish to have between maneuvers. This time, τ , can be chosen to be that time between drift rate corrections using the conventional approach in the absence of eccentricity considerations.⁴ If the control box is $\pm\Delta\lambda$, then this must be reduced by an estimate of the expected errors in the maneuver (timing, thrust performance, etc.) and the excursion in longitude due to eccentricity in order to determine the drift ΔV needed.

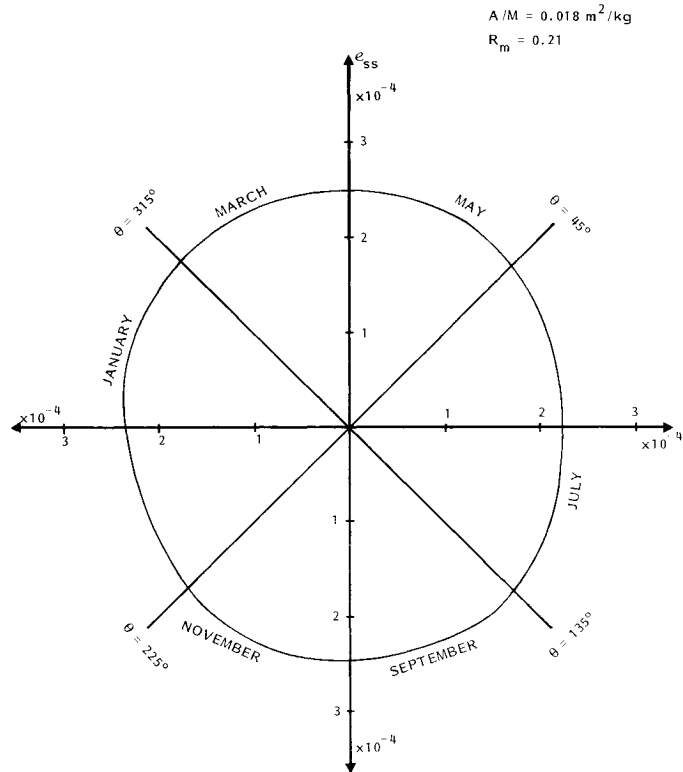


Fig. 8 Annual steady-state eccentricity.

The daily motion due to eccentricity exhibits itself as an oscillation about the daily average position in the form

$$\delta\lambda = 2e(\sin M - \sin M_0)$$

where M_0 is the mean anomaly at the nodal crossing. This produces a maximum daily excursion in longitude of $4e$, with the oscillations about average longitude of $\pm 2e$. Thus, with the limit e_L , the control box becomes

$$\Delta\lambda_0 = \Delta\lambda - 2e_L - \epsilon$$

where ϵ is an estimated effect of control errors (typically 5% of applied impulse; that is, a function of spacecraft hardware performance).

Having determined the maneuver period τ , the change in eccentricity $\delta\vec{e}_\tau$ can be found using the results of the earlier discussion. This function, Eq. (5), must, however, be transformed into the appropriate coordinates. If the solar meridian is $\lambda_s(t_i)$, then the vectorial change becomes

$$\delta\vec{e}(t_i) = \delta e(t_i) \begin{Bmatrix} \cos[\lambda_s(t_i) + \pi/2] \\ \sin[\lambda_s(t_i) + \pi/2] \end{Bmatrix}$$

daily. Consequently, the total vector change over τ days becomes

$$\delta\vec{e} = \sum_{i=1}^{\tau} \delta e(t_i) \begin{Bmatrix} \cos[\lambda_s(t_i) + \pi/2] \\ \sin[\lambda_s(t_i) + \pi/2] \end{Bmatrix} \quad (7)$$

If left unconstrained, the eccentricity at the end of τ days will become

$$\vec{e}_\tau = \vec{e}_0 + \sum_{i=1}^{\tau} \delta\vec{e}(t_i)$$

With the limit on eccentricity, the vector \vec{e}_L is chosen to be

$$\vec{e}_L = e_L \hat{e}_\tau \quad (8)$$

that is, the limiting eccentricity points in the direction of the final unconstrained motion. Thus, the eccentricity necessary to initiate the cycle is

$$\vec{e}_1 = \vec{e}_L - \sum_{i=1}^{\tau} \delta \vec{e}(t_i) \quad (9)$$

The change in eccentricity is

$$\Delta \vec{e} = \vec{e}_0 - \vec{e}_1 \quad (10)$$

and the total velocity change becomes

$$\Delta V_e = V_s \Delta e / 2 \quad (11)$$

Using conventional drift rate control, the drift rate that initiates the cycle is $\dot{\lambda}_0$ (rad/day) and the required ΔV is

$$\Delta V_d = |(\dot{\lambda}_0 - \dot{\lambda}_1) / n| V_s / 3 \quad (12)$$

with n the mean orbital motion and $\dot{\lambda}_1$ the drift rate prior to the maneuver.

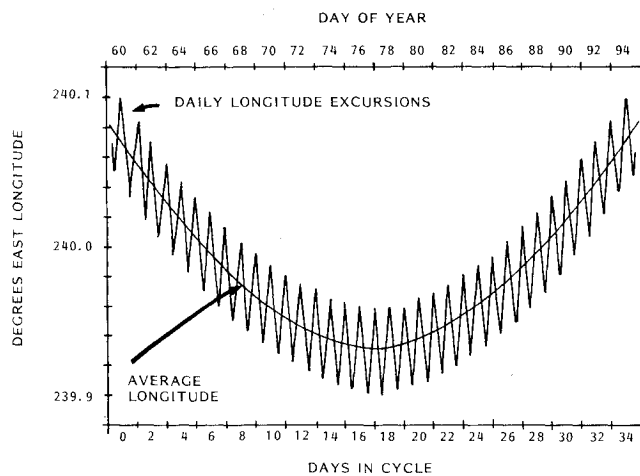


Fig. 9 Optimal drift cycle in the absence of luni-solar gravitational perturbations.

In order to accomplish the desired control, an unbalanced Hohmann transfer is used, where the magnitude of the velocity difference between the two parts is the drift rate correction velocity from Eq. (12).

Thus, a control scheme, Eqs. (7-12), has been developed that provides the desired effect: 1) constrains eccentricity, and 2) east-west stationkeeping. It should be noted that, in many cases, the velocity change will be less than that for conventional east-west stationkeeping where eccentricity is left unconstrained.

As an example of this technique, a typical drift maneuver cycle for a spacecraft is examined. Taking the example of a momentum bias spacecraft ($A/m = 0.018 \text{ m}^2/\text{kg}$, $R_m = 0.21$), Fig. 7 can be utilized to develop the steady-state eccentricity e_{ss} as a function of time of year, as has been done in Fig. 8. As can be seen, there are slight variations in e_{ss} , from 0.000254 to 0.000224 throughout the year. The use of the maximum value of e_{ss} as e_L and a nominal control box of ± 0.1 deg, produces a usable control regime of ± 0.071 deg.

If the nominal station is 240°E longitude, then it is possible to calculate the drift cycle utilizing $\Delta \lambda_0 = 0.071$ deg. From Ref. 4, the initial drift rate is -0.015 deg/day and exhibits a maneuver cycle period of approximately 34 days. Figure 9 is a plot of this drift cycle using only terseral and zonal harmonics with the effects of eccentricity superimposed. As is evident, at no time does longitude violate the stationkeeping limits. If the full limit (± 0.1 deg) had been used, longitude would have violated the limits about half the time during the several days it is near the boundary.

Large Platforms

While the above approach is useful for communication satellites that are typically used by the industry, it will not work for the large geostationary platform under consideration by NASA, unless the longitude control regimes are relaxed to nearly 1 deg.⁵ This would then require some very complicated beam steering mechanisms to give the appropriate signal response for each payload. An alternative, and perhaps cheaper, approach to this follows.

The projected cross-sectional area of these platforms is about 1400 m^2 with a mass of 8200 kg . The resultant daily change in eccentricity as a function of time of year appears in Fig. 7. The values indicated are up to 10 times anything ex-

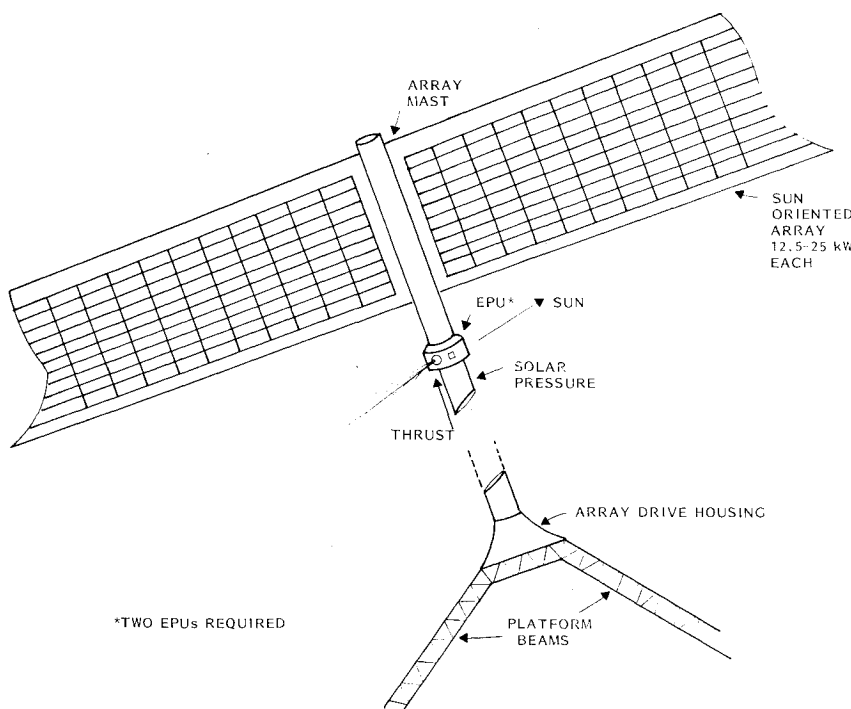


Fig. 10 Platform eccentricity control features.

Table 3 Properties of electric propulsion units (EPU's)^a

Powerplant specific weight	30 kg/kW projected
Impulse	2.2 × 10 ⁶ N-s each 4.4 × 10 ⁶ N-s total
Critical exhaust velocity	1.78 × 10 ⁵ m/s each
Optimum exhaust velocity	1.24 × 10 ⁵ m/s each
Specific impulse I_{sp}	12,670 s each
Efficiency	0.5 estimated
Power	600 W each
Propellant mass	35.4 kg total
Thrust	4.7 mN each

^aTwo units are required.

perienced in the past and, as stated, make control difficult. The best approach to eccentricity control, therefore, would be to counter the motion at all times.

The force upon a satellite of this type is about 9.3 mN. Thus, it is necessary to provide this thrust in the opposite direction to eliminate eccentricity from a control consideration.

This particular platform has as a design feature solar arrays providing at least 25 kW of power; consequently, an electric propulsion unit (EPU) could be used. Thus, when entering the eclipse seasons, the EPU would shut itself down upon entering the shadow, and provide no thrust—as would be required. In order to provide the necessary thrust direction, the EPU would be mounted as an integral part of the array, with the exhaust opposite to the sun. Additionally, two such units would be necessary, each symmetric with the platform's center of mass. This feature is illustrated in Fig. 10.

Using the total mission impulse requirements for the typical 15-yr mission, and the estimated specific weight for future solar arrays, it is possible to characterize the EPU's.⁶ Table 3 is a summary of the required properties. The use of the EPU's would then allow conventional stationkeeping to be implemented.

Conclusion

It has been shown that, under the small longitude control boxes coming into vogue with geosynchronous communication satellites, eccentricity must be constrained. By using the method of perturbations, the relation between solar pressure and eccentricity has been derived. The theory accounts in an accurate manner for the annual variations due to the Earth's orbit about the sun and the various material reflectivities used upon a satellite. Using this theory, an examination of representative behaviors for a variety of spacecraft types is possible to illustrate the effects.

A method has been derived utilizing the solar pressure perturbations that allows simultaneous control of eccentricity and drift rate. This will maximize the time between maneuvers to the limit of ideal conventional east-west stationkeeping.

An examination is made of this effect upon large geosynchronous platforms and a control scheme that utilizes electric propulsion to counter the solar pressure.

References

- ¹Molchoff, N. (Assoc. Ed.), "Technology '80: Communications and Microwave," *IEEE Spectrum*, Jan. 1980, pp. 38-43.
- ²Brouwer, D. and Glemence, G.M., *Methods of Celestial Mechanics*, Academic Press, New York, 1961, p. 45.
- ³McGlinchey, L.P. and Rose, R.E., "Pointing and Control of Planetary Spacecraft—The Next 20 Years," *Astronautics & Aeronautics*, Vol. 17, Oct. 1979, pp. 36-43.
- ⁴Kamel, A., Ekman, D., and Tibbits, R., "East-West Stationkeeping Requirements of Nearly Synchronous Satellite Due to Earth's Triaxiality and Luni-Solar Effects," *Celestial Mechanics*, Vol. 8, 1973, pp. 129-148.
- ⁵Covault, C., "Platform Designed for Numerous Uses," *Aviation Week and Space Technology*, June 19, 1978.
- ⁶Loh, W.H.T. (Ed.), *Jet, Rocket, Nuclear, Ion and Electric Propulsion: Theory and Design*, Springer-Verlag, New York, 1968, pp. 427-462.